CHALMERS

A Volume of Fluid-Based Approach for Investigation of Interaction between a Solid Particle and a Bubble

Master of Science Thesis

Ebrahim Karimi Sibaki

Department of Chemical Engineering

Division of Chemical Reaction Engineering

CHALMERS UNIVERSITY of TECHNOLOGY

Göteborg, Sweden, 2010

A Volume of Fluid-Based Approach for Investigation of Interaction between a Solid Particle and a Bubble

Ebrahim Karimi Sibaki

Supervisors:

Henrik Ström

Department of Chemical Engineering

Division of Chemical Reaction Engineering

Srdjan Sasic

Department of Applied Mechanics

Division of Fluid Dynamics

Master of Science Thesis

Abstract

Bubbles and particles frequently interact in different multiphase processes. Froth floatation, ion floatation, foam fractionation, waste water treatment, foam separation of proteins are only several examples of separation processes in which this interaction has the key role and millions of tons of material are treated annually. Many industries release lots of sewage metal ions into natural water of environment contains lots of metal ions which are not only rare and valuable but also toxic. Then bubbles are used to separate them. In summary, the interaction is of great importance and, as such, it will be the topic of the present work.

The objective of this thesis is to do a direct numerical simulation based on the Volume of Fluid method to investigate the behavior of a bubble and a particle throughout interaction. Several cases are going to be demonstrated to study the influence of separation distance on the particle and the bubble trajectories.

The drag force of the particle throughout interaction with a bubble was described by hydrodynamic resistance functions. They are derived by Nguyen (2007) for non-deformable interface in creeping flow. The results from our simulations are compared to the analytical model of Nguyen. Moreover, hydrodynamic resistance functions for a flattened bubble whit a deformed interface are computed and compared to the non-deformable interface.

One of the main parameters to characterize the interaction is Collision (Encounter) efficiency. Several models are proposed for evaluation of collision efficiency and grazing radius and they are based on a number of assumptions. A comparison is made between the obtained information from the models and the results from our simulations to find the best approximation for grazing radius and collision efficiency.

At the end, several cases for interaction between a deformed bubble and a solid particle are illustrated.

Acknowledgements

Contents

Introduction

Bubbles and particles frequently interact in a large number of multiphase processes, such as froth flotation and antifoaming [1]. In those processes, bubbles are used to extract useful components of ore from gangue where reagents that are recognized by collectors and frothers are added to bubbles. Then these contaminated bubbles are employed in pulp flotation [2].In addition, adhesion of solid particles to bubbles often leads to improvement of mass transfer. For instance, collisions of catalyst particles to bubbles enhance mass transfer and increase rate of reaction in a stirred slurry reactor [3]. Also, many industries release a great deal of sewage into rivers and lakes. Such an environment then contains plenty of metal ions that are not only rare and valuable but also toxic. Then we can use bubbles within the separation process. As an example, zinc and cadmium cations in the presence of ferric and aluminum hydroxides are separated by adsorptive bubbles [4]. Behind all these processes is the phenomenon of creation of agglomerates consisting of particles and bubbles. The goal is that particles are attached to the bubbles and then rise together through a suspension. Finally the created agglomerates are, afterwards skimmed off from the surface of the suspension. . Figure1 shows agglomeration of coal particles and a bubble [5]. Froth flotation, ion flotation, foam fractionation, waste water treatment, and foam separation of proteins are only several examples of such separation processes in which millions of tons of material are treated annually [6]. In summary, the Interaction is of great importance in many industries and, as such, it will be the topic of the present work.

Figure 1: Agglomeration of coal particles and a bubble, (B. Albijanic (2010) [5])

Agglomeration

Successful attachment of a particle to a bubble depends on the particle size and surface chemistry, hydrophobic and hydrophilic properties of the particle surface as well as forces between bubble and particle [7]. Figure 2 shows existence of some different forces between the bubble and the particle. The forces can be generally divided into surface (interparticle) and hydrodynamic forces [9]. The surface forces are van der Waals and electrostatic forces that are described by DLVO theory of Derjaguin (1948) [8]. They become significant when the distance between bubble surface and particle surface is very low, typically 100 nanometer [6]. The drag force, gravity, and buoyancy are the main components of the hydrodynamic forces.
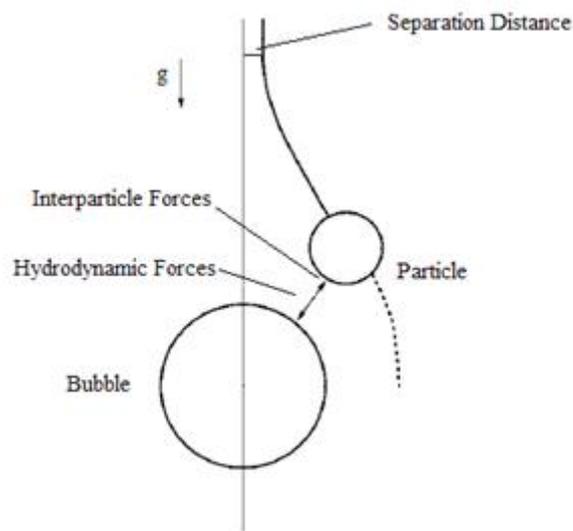
Figure 2: Approaching of a rising bubble and a falling particle

Creation of an agglomerate is a very complex process. Due to the gravity force, the particle is falling and the bubble is rising. As particle approaches the bubble surface, it is slowed down since the intervening liquid between the bubble surface and the particle surface resist becoming thin [11]. The entire attachment process can be explained by three different times. First, the induction time which is required time for the intervening liquid to become thin to form a film at critical thickness. Second, rupture time which is required time for the film to rupture and form a three phase contact line. Third, three phase contact line time which is required time for expansion of contact line to form a stable wetting perimeter [5]. In order to have a successful attachment, the contact time which is the sum of the induction and the rupture time must be less than the attachment time [5]. Figure 3 shows attachment of a solid particle to a bubble.
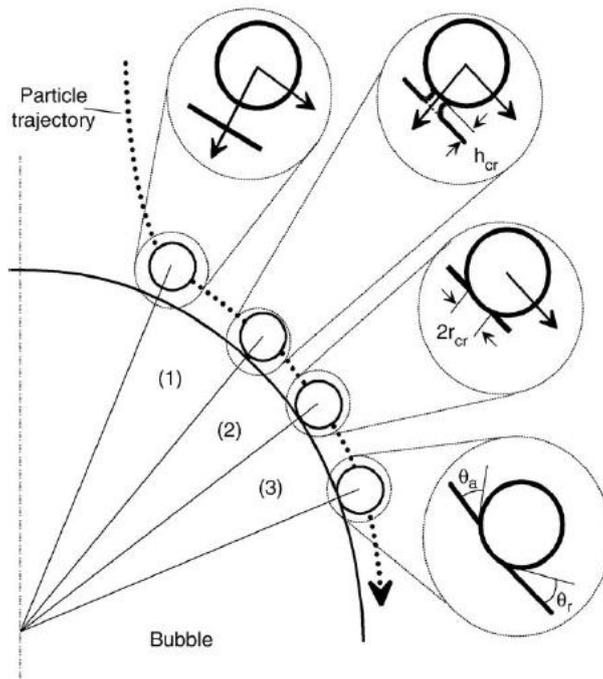
Figure 3: Schematic representation of bubble-particle attachment [5]

Bubble treatment is different in presence of a hydrophobic particle or a hydrophilic particle. Usually, for a hydrophilic solid particle, the liquid film between the particle and the bubble remains stable and no attachment happens. In contrast, for a hydrophobic particle the liquid film is ruptured and the particle attaches to the bubble [11]. It is still a controversy that rupturing of the film is due to a phenomenon or a force called long range hydrophobic force. Rupturing of the film was explained by a physico-chemical phenomenon. For a hydrophobic particle, there are several thousand nano bubbles trapped at the surface of the particle. At critical thickness distance between bubble surface and particle surface, coalescence of nano bubbles create a hole inside the intervening film results in sudden rupturing of the film and formation of a bulge for the bubble [11]. The bubble shape in this situation is called bottleneck. For a hydrophilic particle, the film remains stable and a dimple is formed. This phenomenon called flattening of the bubble in presence of a hydrophilic particle. Figure 4 shows dimple and bulge formation throughout interaction of a hydrophilic and a hydrophobic particle with a bubble [12].

Figure 4: A) Dimple formation of the bubble in presence of a hydrophilic particle (Flattening). B) Bulge formation of the bubble in presence of a hydrophobic particle (Bottleneck).

In the current work, a new framework based on the Volume of Fluid (VOF) method is proposed for investigation of interaction between a solid particle and a bubble. Handling arbitrary sizes of the bubble and the particle is the advantage of this framework. Besides, shape and trajectory of the bubble and also trajectory of the particle can be tracked throughout interaction. Only hydrodynamic forces are taken into account and several cases with different separation distances are demonstrated to investigate the influence of separation distance on the particle and the bubble trajectories. The drag force of the particle throughout interaction with a bubble is modified by hydrodynamic resistance function which is explained in next section.

Hydrodynamic Resistance Functions

Hydrodynamic interaction between a bubble and solid particles strongly affect attachment of particles to the bubble in several processes such as flotation [13]. Strong hydrodynamic interaction between a bubble and a particle may result in no attachment even in presence of hydrophobic particle and attractive surface forces e.g. van der Waals forces [9].

Axisymmetric approach of a solid particle to a bubble was modeled by Nguyen (2002) for short-range hydrodynamic interaction that stream function for liquid flow disturbed by the particle was derived and then employed to calculate hydrodynamic forces on the particle. In addition, Stokes regime was assumed for undisturbed flow of liquid close to the bubble surface [14]. Nguyen (2005) extended his model for sliding particles on a rising bubble [15]. His model agrees with experimental trajectories of latex particles.
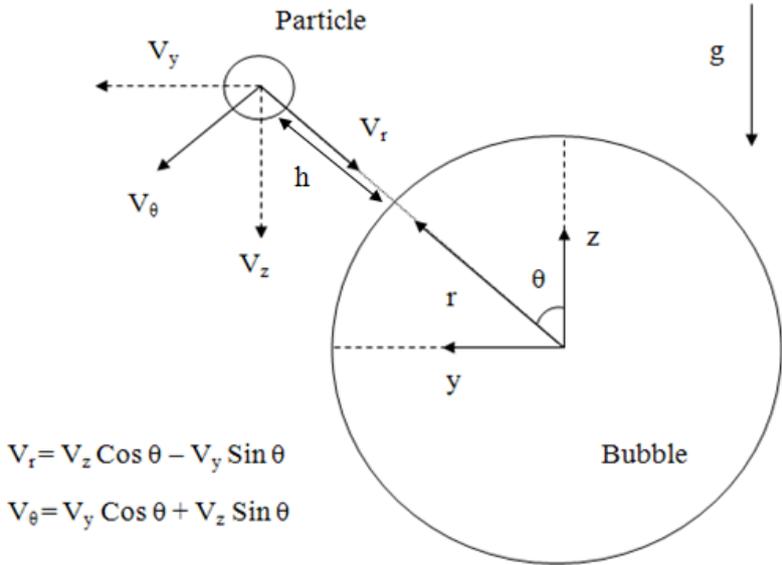
Figure 5: Schematic representation of radial and tangential velocities of the particle

The following equations express radial and tangential components of the particle drag force [16] which is shown in figure 5.

$$\tag{1}$$

$$\tag{2}$$

Where   is particle radius,   is liquid viscosity,   and   are radial and tangential velocities of the particle,   and   are radial and tangential velocities of surrounding fluid, , , , and   are hydrodynamic resistance functions, and   ,   are radial and tangential components of the particle drag force approaching a bubble.

Nguyen assumed that the particle size (typically 10 μm) is significantly smaller than the bubble size (typically 1 mm) and the local geometry of the bubble can be approximated to be a plane. Furthermore, deformation of the bubble surface during interaction is insignificant and liquid flow close to the bubble surface is creeping [15]. Then Resistance functions were calculated for slip and no-slip interface of the bubble. Summary of Nguyen's model for resistance functions are described in table 1 where h is distance between bubble surface and particle surface and (h/r_p) is dimensionless distance [16].

No-slip Interface	Slip Interface

Table 1: Hydrodynamic resistance functions [16].

Collision Efficiency

Collision (Encounter) efficiency is one of the main parameters to characterize interaction. This parameter strongly depends on the surface forces e.g. Van der Waals force as well as hydrodynamic forces between particles and the bubble [13]. The collision efficiency is defined as the ratio of the real collision rate to the ideal collision rate. Ideal collision rate is described by the rate of transferred particles in vertical direction by a bubble and the real collision rate is expressed by particle concentration in a unit volume of liquid together with relative velocity of the particle and the bubble [17]. Weber and Paddock (1983) defined Collision efficiency as the ratio of the number of particles colliding with the bubble to the number of swept particles across the bubble projected area in unit time [18].

Particle collides with the bubble for sufficiently low initial separation distance. In fact, there is a critical separation distance where for separation distance lower than this critical value, particle and bubble always collide. Figure 6 shows critical separation distance which is also called grazing radius. Equation (3) describes collision efficiency as a function of grazing radius where   is grazing radius and   and   are particle and bubble radiuses respectively [19].

$$\overline{\rule{2cm}{0pt}} \tag{3}$$
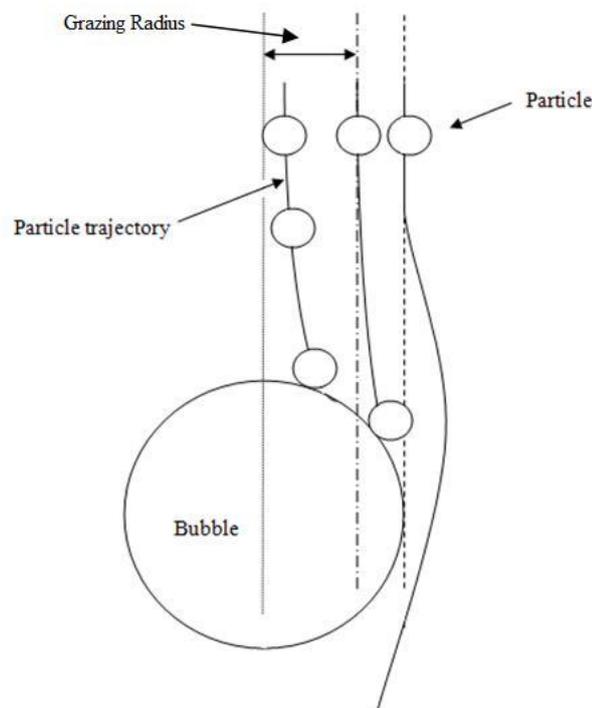
Figure 6: Schematic representation of grazing radius

Several models were proposed for evaluation of collision efficiency and grazing radius. The models were described and discussed in a comprehensive review paper written by Zongfu Dai (2000) [20]. The first attempt to develop a collision model was made by Sutherland (1948) assuming potential flow regime at the bubble surface. Then, collision efficiency was calculated by the ratio of the cross-sectional area of the stream tubes to the projected area of the bubble [20].It is given by equation (4) where   and   are particle and bubble diameters respectively.

$$\overline{\qquad} \tag{4}$$

The grazing radius for Sutherland model is given by equation (5).

$$\overline{\qquad} \tag{5}$$

Gaudin (1957) assumed Stokes flow regime at the bubble surface and ignored the inertial forces of the particle and then suggested the following simple equation to express the collision efficiency [22].

$$\text{-} \, \overline{\qquad} \tag{6}$$

Sutherland model was improved by Dukhin (1983) and inertial forces were taken into account [23]. Generalized Sutherland equation (GSE) is an extended version of Dukhin model which had been proposed by Zongfu Dai (1998) [24]. The collision efficiency was described by a complex function (eq. 7) in GSE model.

$$\overline{\qquad\qquad} \tag{7}$$

$$\overline{\qquad} \tag{8}$$

$$\overline{\qquad} \tag{9}$$

$$\overline{\qquad} \tag{10}$$

Where   is angle of tangency, U is the bubble slip velocity relative to the surrounding liquid, μ is liquid viscosity, ρ and δ are particle and surrounding liquid densities, and   is drag correction which is equal to one based on Dukhin's model (1983). Zongfu Dai (1998) changed drag correction value to   =2 [24].

Nguyen (2009) included the effect of buoyancy and particle density in the particle inertial motion around an air bubble and then solved the equation numerically. It is shown that the drag correction must be equal to one for GSE model [25], [26].

Solution method

The Volume of Fluid (VOF) method is the framework employed to solve the problem considering a three-phase flow of Newtonian, incompressible, and immiscible fluids. This method was proposed by Hirt and Nichols (1981) [27]. Using VOF for a solid particle needs some extra considerations and assumptions that will be discussed after introducing VOF governing equations. The volume fraction of   phase in each computational cell is denoted as   (=1-3). For the cells only filled by phase 1, α_1 is equal to one and for the cells occupied by the second or the third phase, α_1 is equals to zero. If a cell is filled by two or three phases the average value must be used for density and viscosity that are given by the following equations.

$$\qquad (11)$$

$$\qquad (12)$$

Liquid (=1), Bubble (=2), Particle (=3),

The continuity (eq. 13) and momentum (eq.14) equations are used to determine velocity field.

$$\qquad (13)$$

$$\qquad (14)$$

F_σ in the momentum equation represents the surface tension force, and is calculated using the continuum surface tension force (CSF) of Brackbill (1992)

$$\qquad (15)$$

Where σ is the surface tension coefficient between phases, and   is gradient of α [28].

The interface between two phases is tracked by solving the advection equation for the volume fraction of phases in each computational cell that is expressed by the following equation.

$$\qquad (16)$$

The stokes drag [29] on a solid particle is

$$\qquad (17)$$

The stokes drag on a fluid particle based on Hadamard (1911) [30], and Rybczynski (1911) [31] equation is given by

$$\qquad\qquad\qquad \overline{\qquad} \qquad\qquad\qquad\qquad\qquad\qquad\qquad (18)$$

Where, Kappa value (κ) is the viscosity ratio between the two fluids.

Using large kappa value (   ) in equation (18) enables us to simulate motion of a solid particle. Moreover, Capillary number (—) must be small to avoid distortion of the particle. The role of σ for the particle is to keep the spherical shape and also to prevent distortion of that. In conclusion, to model a solid particle within VOF framework, selected viscosity and surface tension of the solid particle must be as large as possible. For further discussion see H. Ström (2010) [32].

Table 2 describes different parameters that are used for simulation. Note that, two different densities are chosen for the particle to show various behavior of the bubble throughout the interaction.

Computational grid size (mm)	0.5×0.5×0.5
Number of cells in the domain (Original mesh)	477744
Number of cells in the domain (Fine mesh)	767936
Time step size (sec)	1×10^{-6}
Liquid Density (kg/m^3) (Water)	1000
Liquid Viscosity (pa.s)	0.001
Bubble Diameter (μm)	130
Particle Diameter (μm)	50
Light particle Density (kg/m^3) [Latex]	2600
Heavy particle Density (kg/m^3) [Copper]	8978
Particle kappa value	10000
Particle surface tension (N/m)	10^{-8}

Table 2: parameters used for simulation of the interaction

In the current work, the advection technique to discretize equation (16) is the Compressive Interface Capturing Scheme for Arbitrary Meshes (CICSAM) [33]. Discretization Schemes for pressure and momentum are PRESTO! and QUICK. Moreover, the pressure-velocity coupling scheme is PISO [34].

Results and Discussions

In this section, several cases with different separation distances are going to be illustrated to investigate the interaction. Before discussing about the cases, the trajectory and the shape of the bubble in absence of the particle must be studied. Then, the influence of the particle on the bubble shape, trajectory, and velocity throughout interaction can be obtained.

Table 3 describes the required dimensionless numbers to predict the shape and the trajectory of the micro bubble used in our simulation. Terminal velocity is calculated using the Rodrigue's generalized correlation for bubble motion [35].

$$\underline{\quad\quad} = 0.013 \text{ m/s} \tag{19}$$

Where a=1/12, b=1, c=49/1000, d=3/4, and $\underline{\quad\quad} = 1.012$

Bubble Diameter (µm)	130
Bubble Terminal velocity (m/s)	0.013
$\underline{\quad\quad}$	1.69
$\underline{\quad\quad}$	1.7×10^{-4}

Table 3: Parameters used for prediction of the shape and the trajectory of the bubble

According to table 4, at 25 $^{\circ}$C, the micro bubble has rectilinear motion and rises straightly upward in stagnant water [37], [38].

Equivalent Bubble Diameter (mm)	Reynolds Number	Path of Bubbles
0 … 1.34	0 … 565	Rectilinear motion
1.34 … 2.00	565 … 880	Helical path
2.00 … 3.60	880 … 1350	First plane then helical motion
3.60 … 4.20	1350 … 1510	Plane motion
> 4.20	> 1510	Rectilinear motion with rocking

Table 4: path of an air bubble rising in stagnant water at 28.5°C [38]

Weber number indicates the importance of inertia compared to the surface tension force. According to table 5, the micro bubble described in table 3 keeps its spherical shape permanently [36].

(mm)	Weber Number	a/b	Shape of the bubble
0 … 0.83	0 … 0.62	1	Spherical
0.83 … 2.00	0.62 … 3.70	1 … 2	Ellipsoid (No Surface Oscillation)
2.00 … 4.20	3.70 … 5.35	2 … 4	Ellipsoid (With increasing Surface Oscillation)
> 4.20	> 6.35	-	Distorted bubble and spherical cap shaped bubble

Table 5: shape of an air bubble rising in stagnant water at $28.5°C$ [36]

In general, three different separation distances are considered. They are high, low, and zero separation distance that are shown in figure 7. Separation distance is lower and larger than bubble radius in the low and the high separation respectively. Besides, a Particle and a bubble move on the same axis in zero separation distance called axisymmetric. Both the heavy particle and the light particle are tested for axisymmetric interaction. Here are the results.
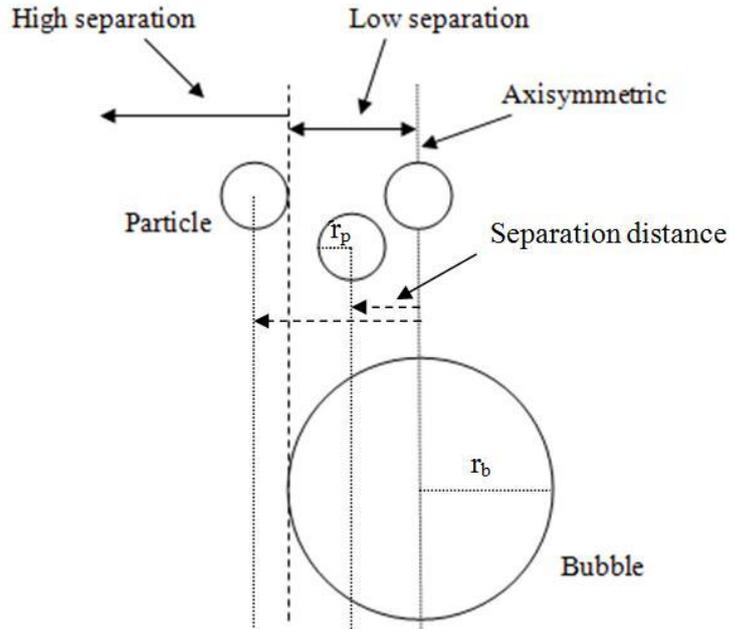
Figure 7: Schematic representation of separation distances

Case 1: Axisymmetric Interaction (Light particle)

Figure 8 shows snapshots of different times for axisymmetric interaction between the bubble and the light particle. Bubble keeps its spherical shape throughout interaction. Particle and bubble velocities are shown in figure 9. A comparison is made between bubble rising velocity in presence of the particle (Interactive Bubble) and in absence of the particle (Free bubble). Apparently, rising velocity of the bubble is reduced due to the interaction. Furthermore, particle velocity is decreased permanently and after 7 milliseconds of flow time, particle direction is changed and it is carried up by the bubble.

Figure 8: Snapshots of different times for axisymmetric interaction (Light particle)

Figure 9: Bubble and particle velocities throughout axisymmetric interaction

In order to compute resistance function, Particle and bubble velocities and for slip and no-slip interface from table 1 are used. Drag force of the particle is calculated by equation of motion for the particle (eq. 20) where is the drag force.

$$\quad\quad\quad\quad\quad\quad\quad\quad\quad\quad\quad\quad\quad\quad\quad\quad\quad\quad\quad\quad\quad\quad\quad\quad\quad\quad\quad\quad\quad (20)$$

Consider that,   and   are equal to zero for axisymmetric interaction since the particle only moves in radial direction. Figure 10 shows comparison of   resistance function for axisymmetric interaction where a very good agreement is observed for no-slip interface.
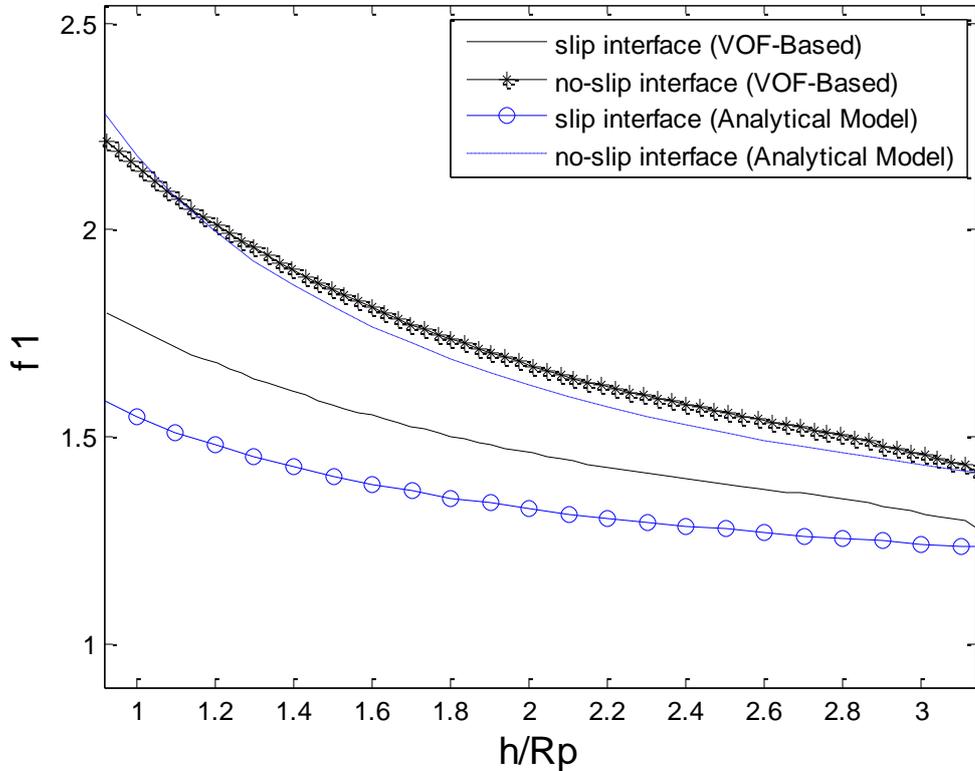
Figure 10: comparison of   resistance function for axisymmetric interaction (Light particle)

Case 2: High separation distance Interaction

Figure 11 shows snapshots of different times for high separation distance interaction. Bubble keeps its spherical shape throughout interaction. Direction of movement for the particle and the bubble at 12 milliseconds shows that they are moving away from each other and no collision happens.
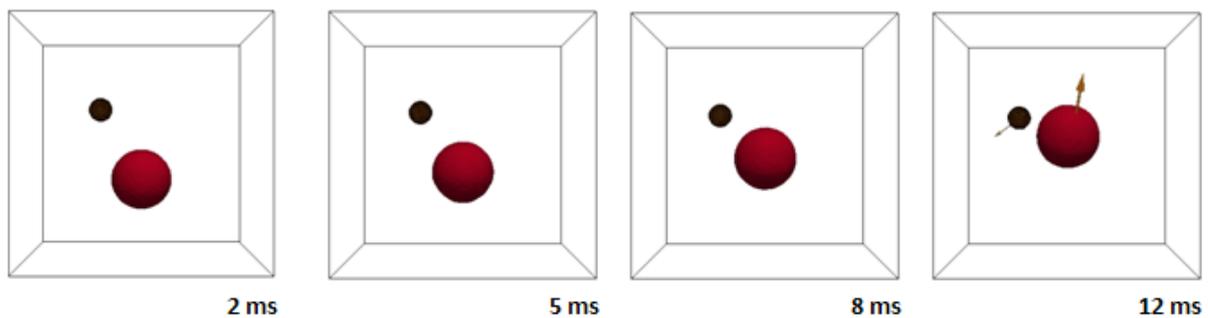
Figure 11: Snapshots of different times for high separation distance interaction

Figure 12 shows velocities of the bubble and the particle. Drift velocity of the particle which means how fast the particle moves in horizontal direction increases to pass the bubble.
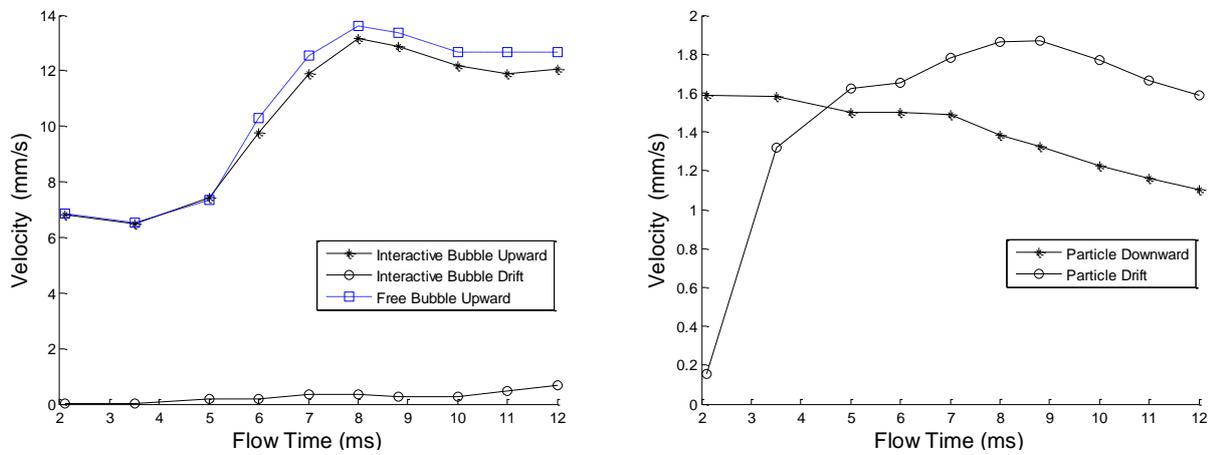
Figure 12: Bubble and particle velocities throughout high separation distance interaction

The same as case 1, hydrodynamic resistance functions are computed. Consider that,   and   are used from table 1 to compute   and   for slip and no-slip interface. Poor agreement is observed between the analytical model of Nguyen and computed   resistance function that shown in figure 14. As mentioned before, it is assumed that particle size is very small compared to the bubble size and the local interface of the bubble is approximated to be a plane by Nguyen (2007). However, In this case, particle size (50 μm) is comparable to the bubble size (130 μm) and assumption of plane interface is no longer valid. Moreover, mesh resolution might be another source of disagreement. The effect of mesh resolution on the simulation results and computed resistance functions will be discussed for low separation distance.
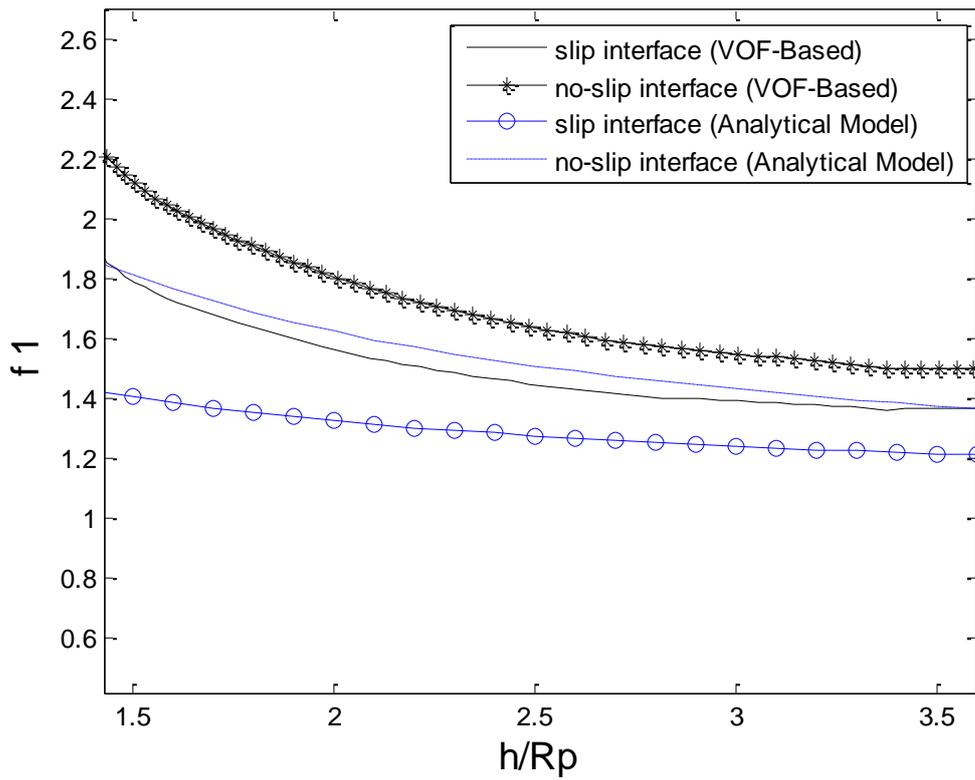
Figure 13: comparison of   resistance function for high separation distance interaction
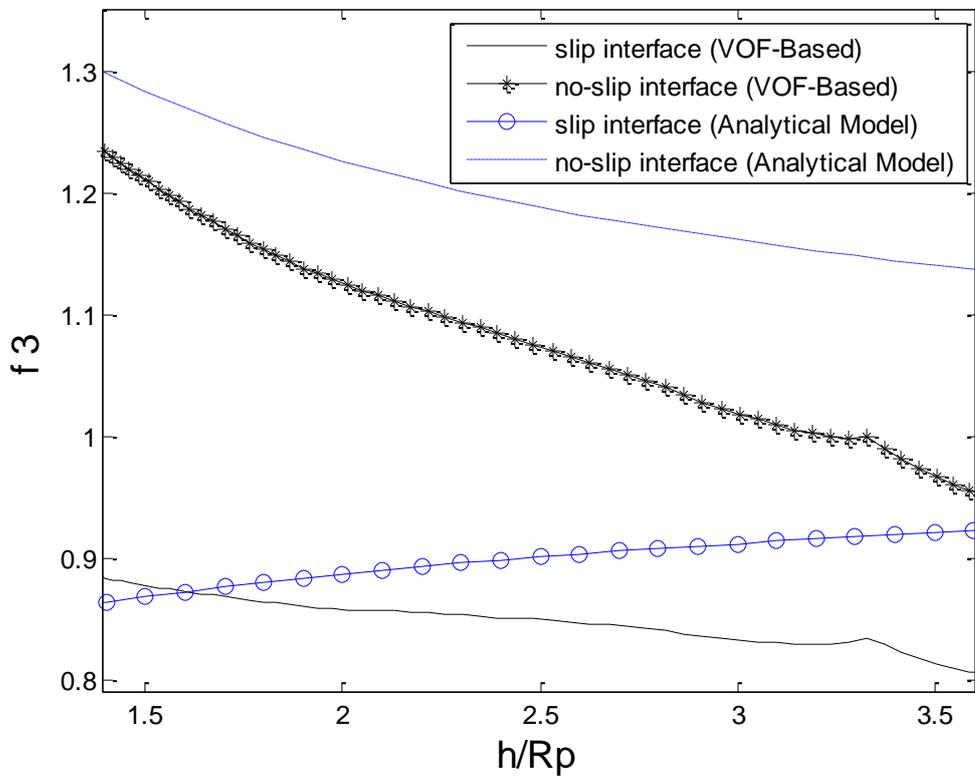
Figure 14: comparison of   resistance function for high separation distance interaction

Case 3: Axisymmetric Interaction (Heavy particle)

For the heavy particle which has large velocity, the particle approaches the bubble and the intervening film becomes very thin. As mentioned before, in this situation, bubble treatment is different in presence of a hydrophobic or a hydrophilic particle. In this work, no hydrophobic effect is defined and the particle is assumed to be hydrophilic. Figure 15 shows snapshots of different times for axisymmetric interaction between the bubble and a heavy particle. Based on figure 16, velocities of the particle and the bubble decrease permanently during interaction.
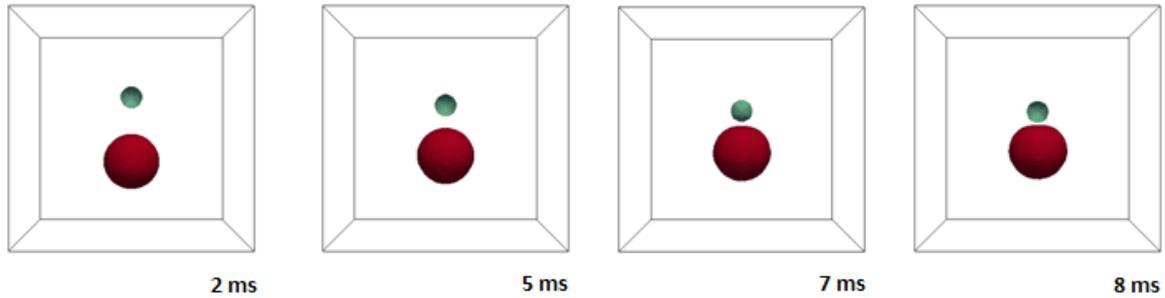
Figure 15: Snapshots of different times for axisymmetric interaction (Heavy particle)

One should consider mesh resolution when the particle and the bubble are very close to each other to measure the depth of deformation for the bubble. Figure 17 shows flattening of the bubble at 8 milliseconds of the flow time when the distance between the particle surface and the bubble surface is one computational cell.
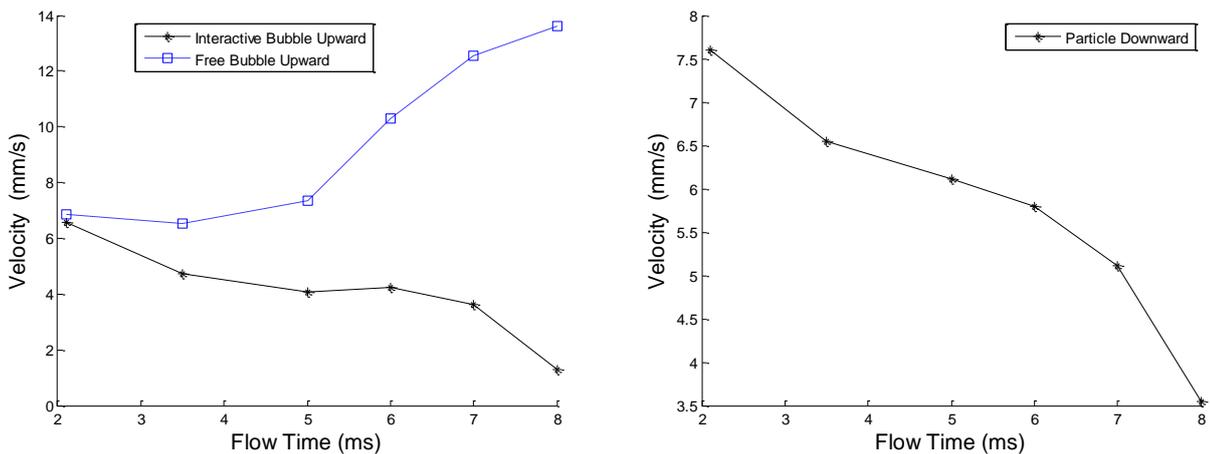
Figure 16: Bubble and particle velocities throughout high separation distance interaction
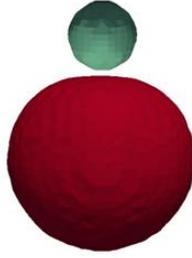
Figure 17: Bubble flattening in presence of a hydrophilic particle

Figure 18 and 19 show comparison of   resistance function between a flattened bubble and a non-deformed bubble for slip and no-slip interface. The resistance function is lower for the flattened bubble than the non-deformed spherical bubble (case 1).

For a deformed bubble during interaction, Part of overall energy among the bubble and the particle is dissipated to deform the bubble called energy of deformation [39], so the contribution of overall energy for the drag force of the particle becomes lower results in lower resistance function.
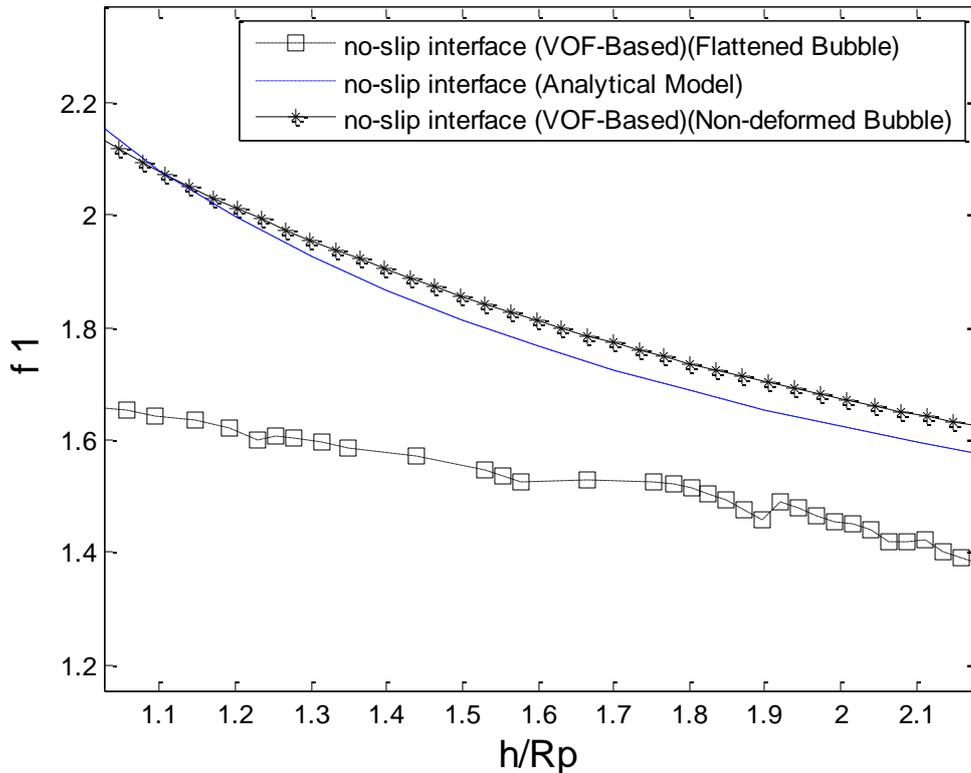
Figure 18: comparison of   resistance function for axisymmetric interaction (Heavy particle) and no-slip interface
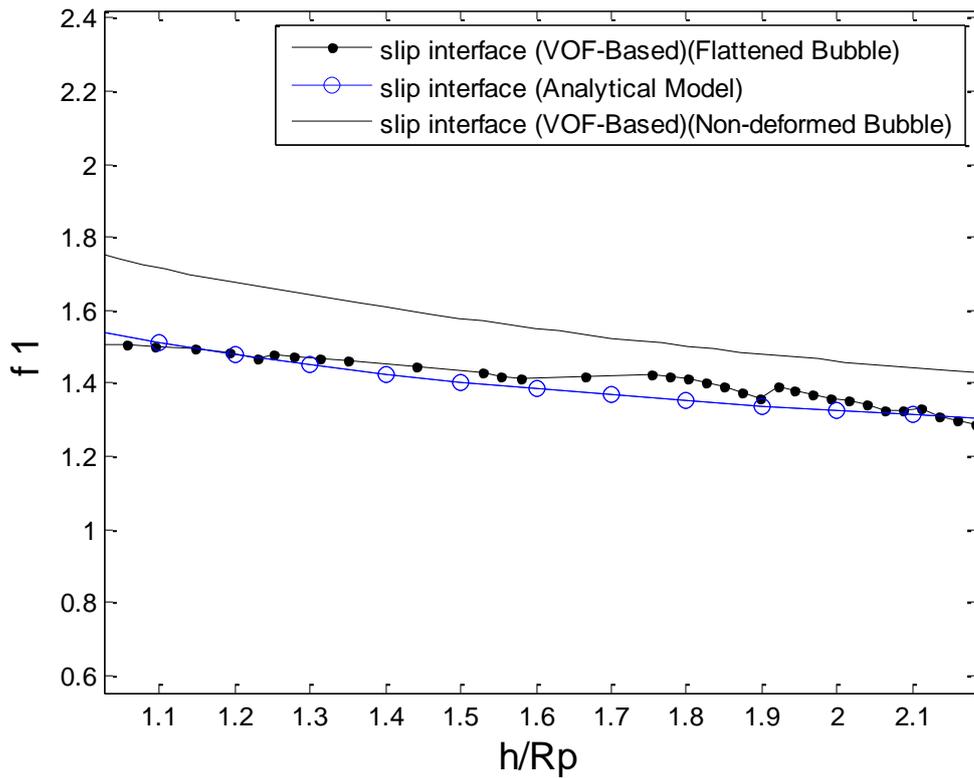
Figure 19: comparison of   resistance function for axisymmetric interaction (Heavy particle) and slip interface

Case 4: Low separation distance Interaction

In this case, particle is located between axis of motion and radius of the bubble (figure 7). Figure 20 shows snapshots of different times for low separation distance interaction where separation distance is 50 μm. particle moves away from the bubble throughout interaction and travels 7 μm horizontally before collision at 12 milliseconds of flow time.

| 2 ms | 5 ms | 8 ms | 12 ms |
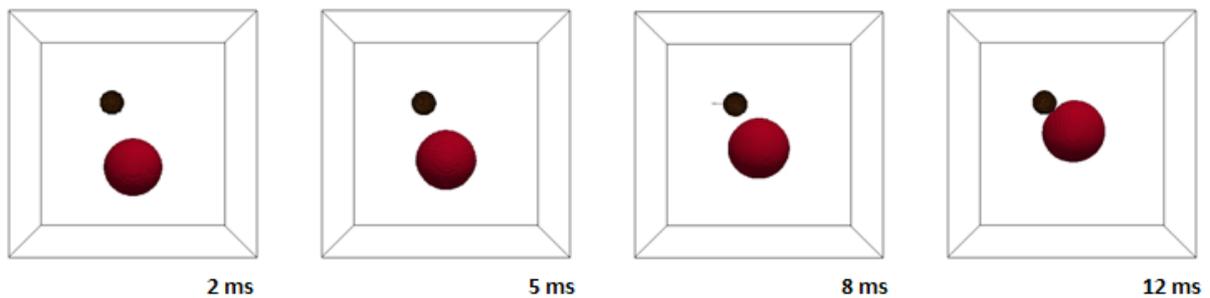
Figure 20: Snapshots of different times for low separation distance interaction

Figure 21 shows velocities of the particle and the bubble throughout low separation distance interaction. Drift velocity of the particle and the bubble increases sharply to avoid collision.
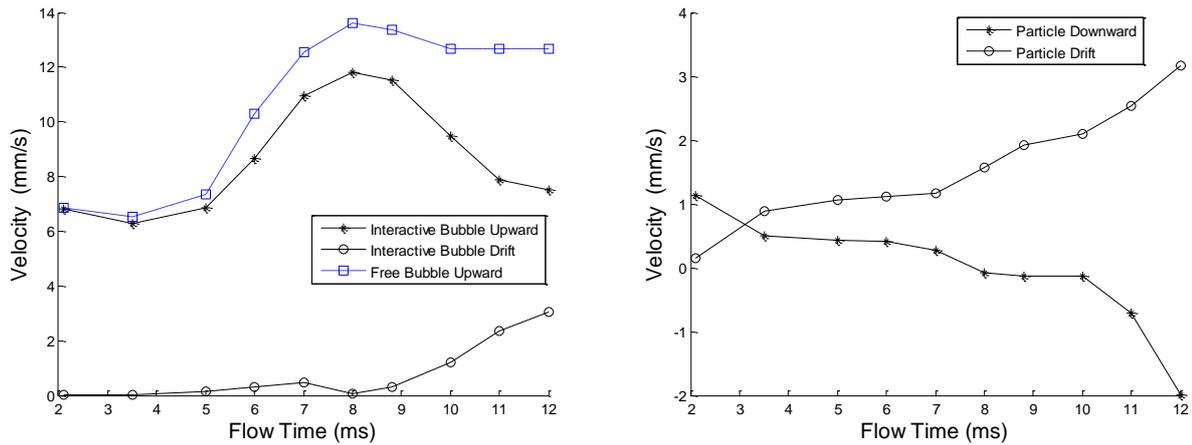
Figure 21: Bubble and particle velocities throughout low separation distance interaction

Figure 22 and 23 show comparison of computed   and   resistance functions with the analytical model where significant deviation is observed for both of them.
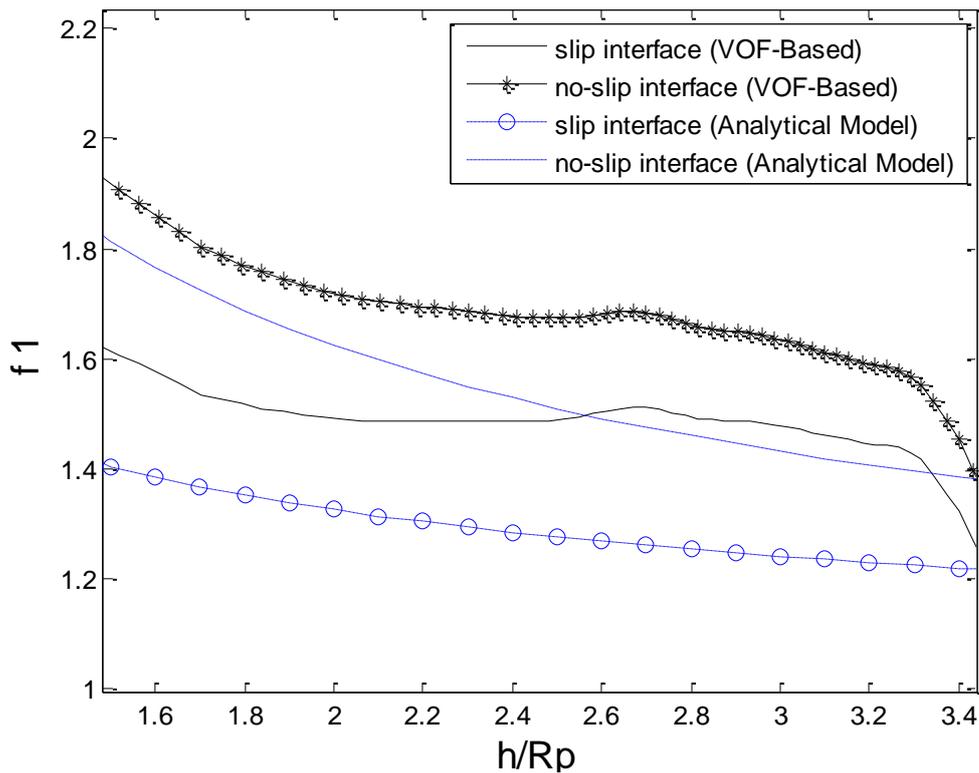
Figure 22: comparison of   resistance function for low separation distance interaction (Original mesh)
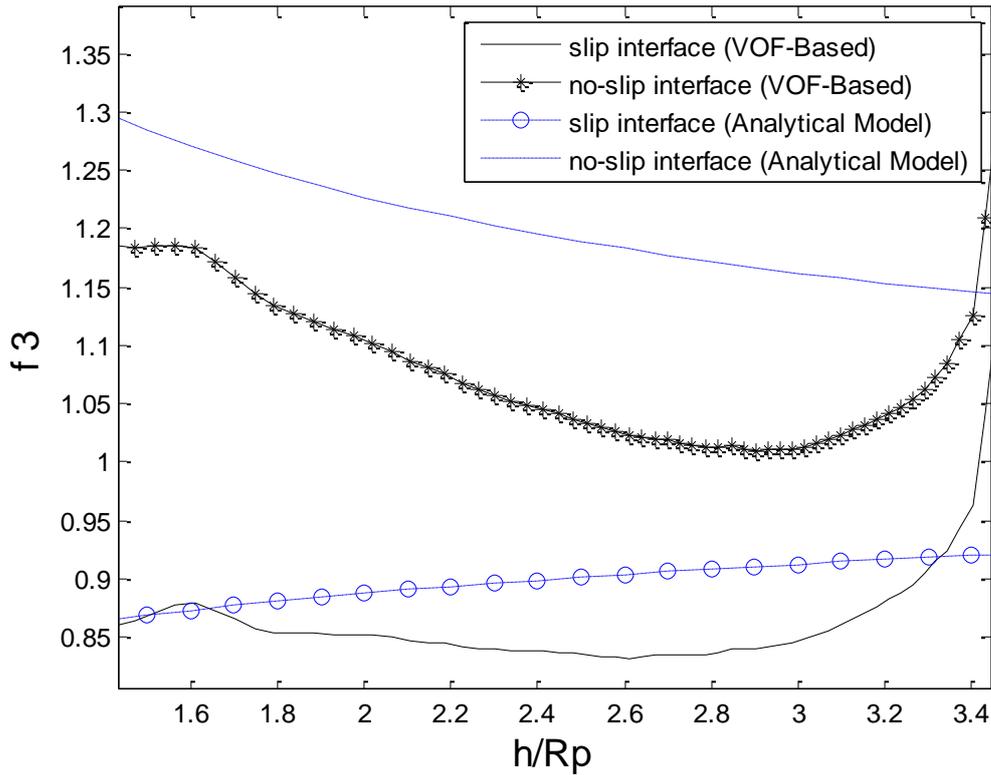
Figure 23: comparison of resistance function for low separation distance interaction (Original mesh)

The simulation is redone in the fine mesh (table 2). Figure 24 and 25 show the comparison of the computed resistance functions with the analytical model for the fine mesh. The resistance functions from the simulation in the fine mesh are corresponding to the analytical model that describes the importance of mesh resolution.

The particle approaches the bubble throughout interaction and the intervening film between them becomes thin. Figure 26 shows the influence of mesh resolution on the film thickness. For the original mesh, the film becomes thinner during interaction until collision happens. In simulations, it is considered that Collision happens once one computational cell inside the intervening film is filled by three phases. Typically surface forces acts when the thickness of the film is around 100 nano meter [6]. For the fine mesh, the minimum observed thickness of the film is around 30 μm which is far from where surface forces acts. Moreover, the particle and the bubble will never collide since the thickness of the intervening film increases after 12 milliseconds of flow time that means they are moving away from each other.
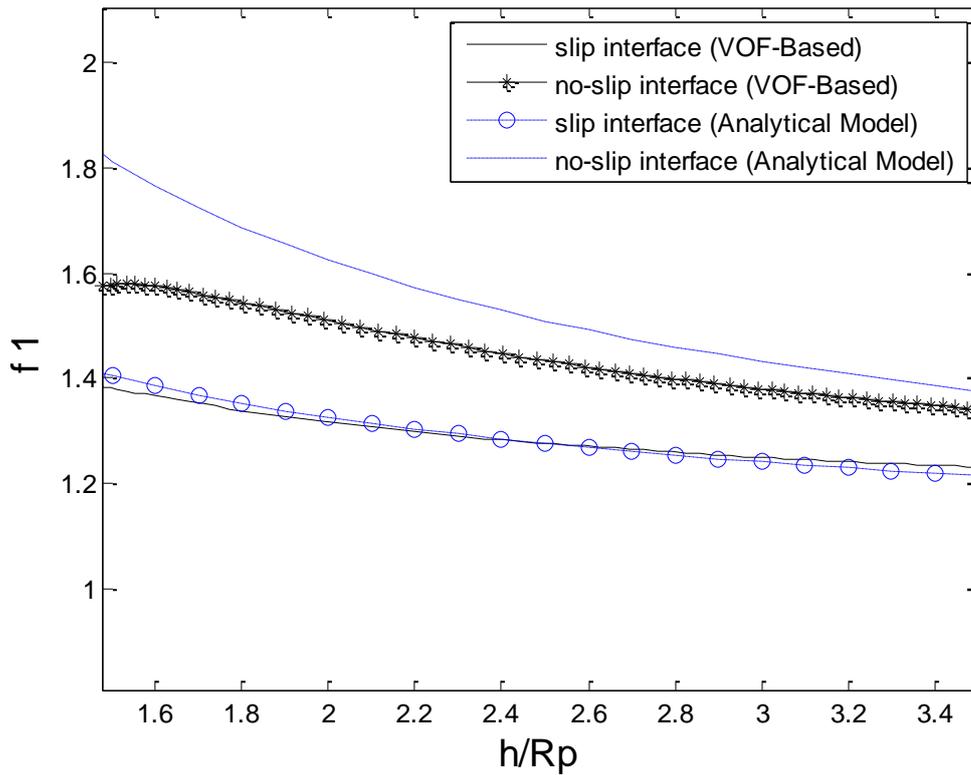
Figure 24: comparison of f_1 resistance function for low separation distance interaction (Fine mesh)
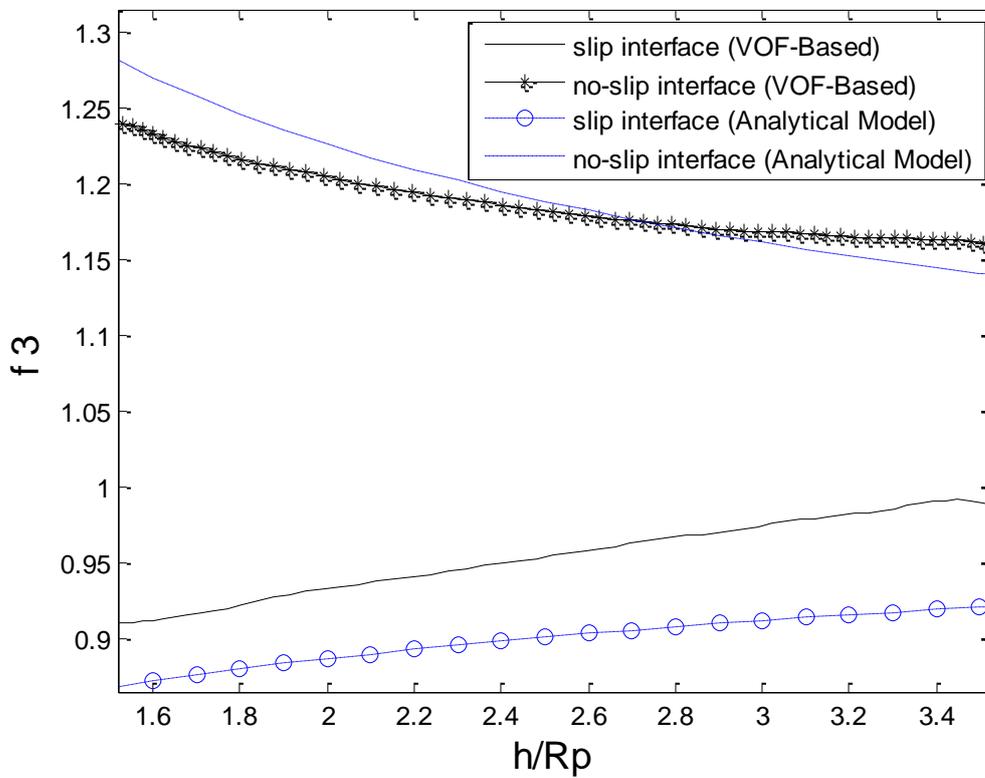
Figure 25: comparison of f_3 resistance function for low separation distance interaction (Fine mesh)
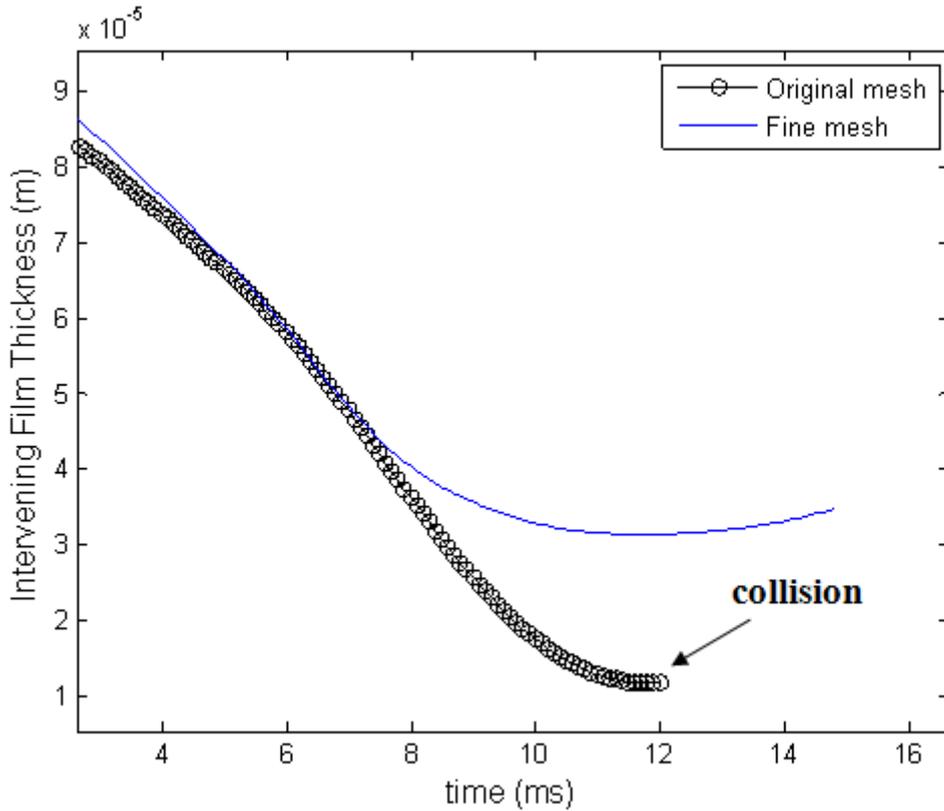
Figure 26: comparison of intervening film thickness for the original and the fine mesh

It is already shown that the particle didn't collide with the bubble for this particular low separation distance (50 µm). It means grazing radius for this size of the particle is lower than 50 µm. Table 6 describes the obtained information from different models.

Models	Collision Efficiency	Grazing Radius (µm)
Sutherland	1.15	70
Gaudin	0.22	42
GSE	0.92	86
Volume of Fluid (VOF)	-	< 50

Table 6: collision efficiencies and grazing radiuses obtained from different models

The inertial deposition of particles on the bubble surface is characterized by the dimensionless particle Stokes number. Stokes number describes the importance of inertial forces compared to the viscous resistance of the intervening film throughout interaction [29]. It is expressed by equation (21) where U is the bubble terminal velocity, µ is liquid viscosity, ρ is particle density, and   and   are particle and bubble radiuses respectively.

$$\overline{} \tag{21}$$

A critical value $\overline{}$ is suggested for the particle Stokes number by Levin (1961) to describe the effect of inertial forces [41]. The value of Stokes number for the simulation is 0.072 which is lower than the critical value. Sutherland model overestimates collision efficiency when the Stokes number is lower than the critical value [20].

According to YOON (1999) investigation on the collision efficiency, Gaudin model agrees with collision efficiency for small bubbles (   ) [42]. In fact, Gaudin model approximates collision efficiency very well for Stokes flow. Simulation results also agree with the Gaudin model since assumption of stokes flow is valid.

Nguyen (2009) showed Generalized Sutherland Equation (GSE) works only for ultrafine particle (< 10 μm) and significant deviation was observed to approximate collision efficiency using GSE model for large particles [25], [26].

Handling Bubble Deformation

As mentioned before, the micro bubble used in our simulations keeps its spherical shape during the interaction. Bubble shape is characterized by Eötvos number (——) and Morton number (——). One way to test bubble deformation during interaction without change of the domain or the bubble size is increasing Eötvos and Morton values using low surface tension for the bubble. In the following cases, surface tension coefficient for the bubble is very low ($\sigma = 10^{-10}$ N/m) and the bubble deforms throughout interaction.

Case 1: Low separation distance

In figure 27, deformation of the bubble results in no collision. According to the direction of movement for the particle at 18 milliseconds of flow time, the particle and the deformed bubble move away from each other. Besides, figure 28 shows the bubble deforms in all directions.

| 2 ms | 7 ms | 13 ms | 18 ms |
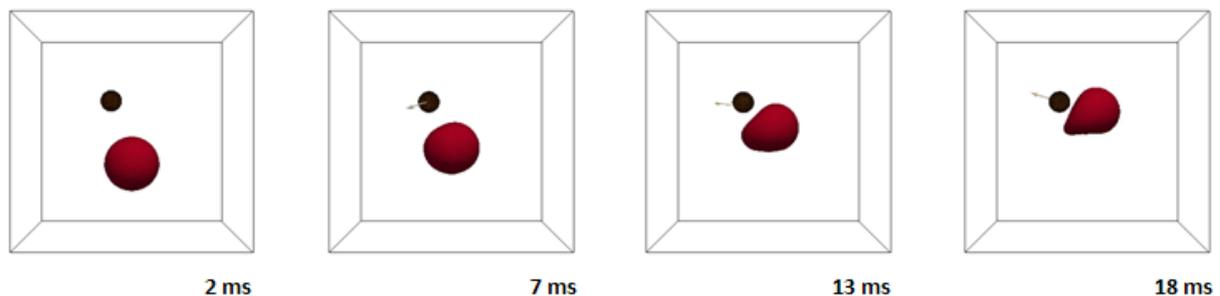
Figure 27: Snapshots of different times of Low separation distance interaction for low bubble surface tension.

18 ms
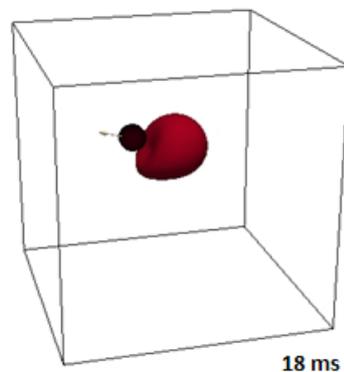
Figure 28: Bubble deformation in all directions

Figure 29 shows change in velocity for the bubble and the particle. The rising velocity of the bubble remains almost constant and its drift velocity is much lower compared to the non-deformed bubble. Moreover, particle starts to rise up after 13 milliseconds of flow time.

Note that, in this case, the entire interaction takes longer time due to deformation of the bubble.
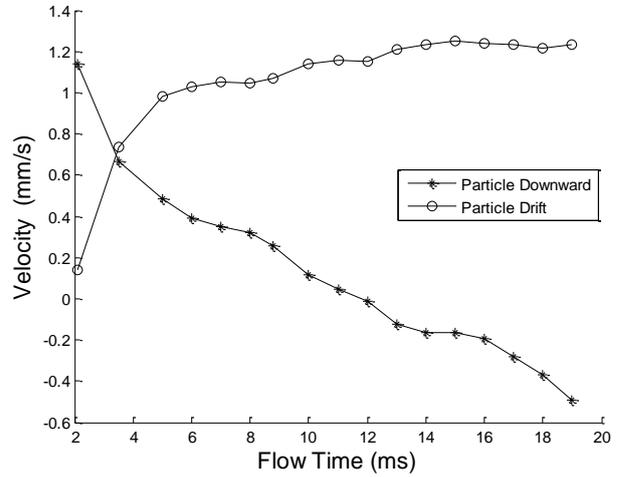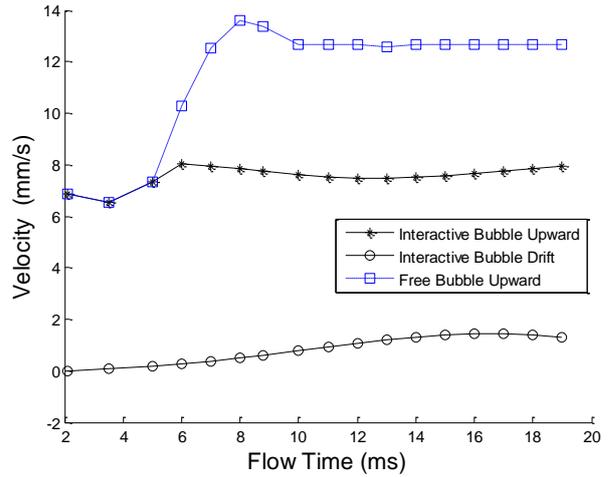
Figure 29: Bubble and particle velocities throughout low separation distance interaction for low bubble surface tension

Case 2: Axisymmetric Interaction (Light Particle)

According to figure 30, the bubble carries up the particle and the intervening film remains stable and no collision happens.
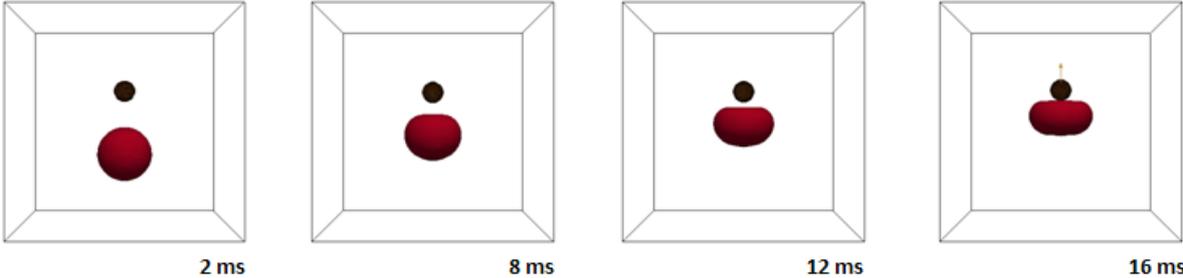
Figure 30: Snapshots of different times of zero separation distance interaction for low bubble surface tension and light particle
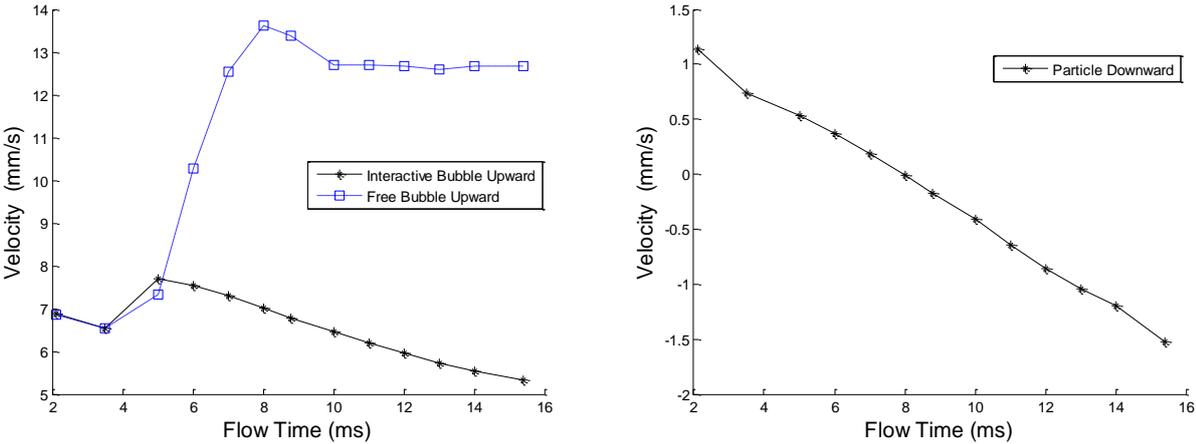
Figure 31: Bubble and particle velocities throughout zero separation distance interaction for low bubble surface tension (Light particle)

Figure 31 shows change in velocity for the bubble and the particle. There is no drift velocity for them since this case is completely symmetrical.

Case 3: Axisymmetric Interaction (Heavy particle)

The heavy particle has large downward velocity and its velocity becomes lower throughout the interaction. Besides, the bubble deforms until it torn apart.
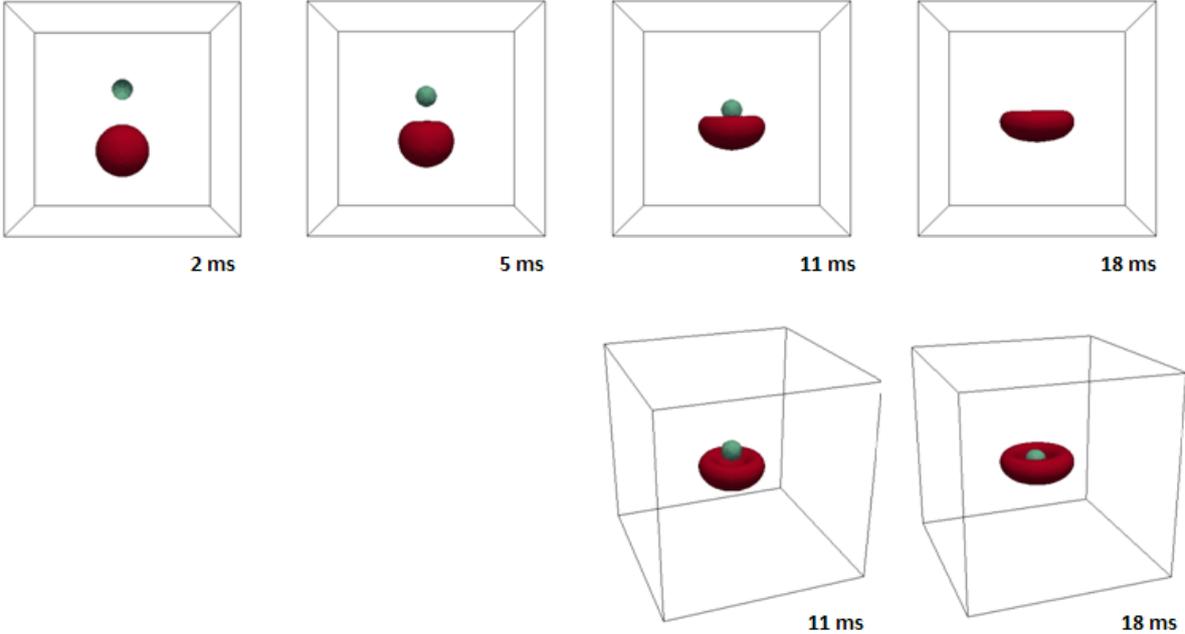
Figure 32: Snapshots of different times of zero separation distance interaction for low bubble surface tension and Heavy particle
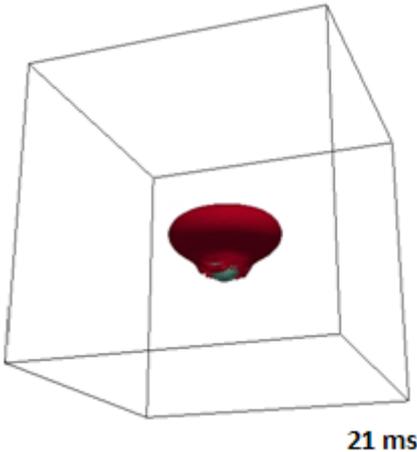
Figure 33: Bubble distortion
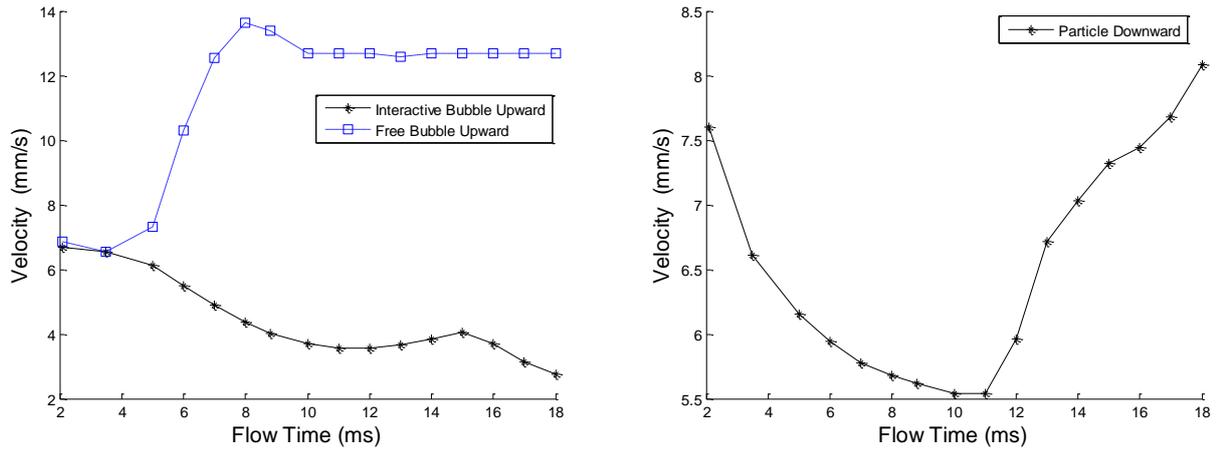
Figure 34: Bubble and particle velocities throughout zero separation distance interaction for low bubble surface tension (Heavy particle)

Figure 34 shows change in velocity for the bubble and the particle. The same as the former case, there is no drift velocity for the bubble and the particle. The velocity of the bubble and the particle decrease permanently. However, after distortion, velocities of the bubble and the particle increase.

Conclusions

A new Volume of Fluid based approach is proposed for investigation of a solid particle and a bubble interaction. Several cases with various separation distances are demonstrated to show the behavior of the particle and the bubble throughout interaction. Simulation results are compared to the analytical model of Nguyen. In addition, hydrodynamic resistance functions for a flattened bubble where the interface is deformed are computed. Several analytical models are proposed to approximate the collision efficiency and the grazing radius of the interaction. Simulation results are compared to the obtained information from the models to find the best approximation. Finally, low surface tension for the bubble is used to demonstrate interaction of a solid particle and a deformed bubble.

References

[1]- F.omota et al., Adhesion of solid particles to gas bubbles.Part2: Experimental, Chemical Engineering science 61 (2006), 835-844

[2]- Leja J. Surface Chemistry of froth flotation. New York: Plenum Press; 1982

[3]- Ruthiya, K.C, et al., Modeling the effect of particle to bubble adhesion on mass transport and reaction rate in a stirred slurry reactor. 2004, Chemical Engineering Science 59, 5551-5558

[4]- Kazimier Jurkiewicz, Adsorptive bubble separation of zinc and cadmium cations in presence of ferric and aluminum hydroxides, Journal of colloid and Interface Science 286 (2005) 559-563

[5]-B. Albijanic, A review of induction and attachment times of wetting thin films between air bubbles and particles and its relevance in the separation of particles by flotation, Articles in press, Advance in colloid and Interface Science (2010)

[6]- K. Malysa et al., Influence of surface active substances on bubble motion and collision with various interfaces, Advances in colloid and interface Science 114-115 (2005) 205-225

[7]- X. Fana et al., Attachment of solid particles to air bubbles in surfactant-free aqueous solutions, Chemical Engineering Science 59 (2004) 2639 – 2645

[8]- Derjaguin, B.V., Landau, L., 1941. Theory of stability of highly charged lyophobic sols and adhesion of highly charged particles in solutions of electrolytes. Acta Physicochim URSS 14, 633–652

[9]- D.M Leppinen, A kinetic model of dissolved air floatation including the effects of interparticle forces, Journal of water supply (2000) 259-268

[10]-A hydrodynamic model for bubble—particle attachment, Journal of Colloid and Interface Science, Volume 154, Issue 1, November 1992, Pages 129-137

[11]- M. Krasowska et al., Wetting films in attachment of the colliding bubble, Advances in colloid Interface Science 134-135 (2007) 138-150

[12]- J. Nalaskowski et al., Study of particle- bubble interaction using atomic force microscopy- current possibilities and challenges, Physicochemical problems of mineral processing 36 (2002) 253-272

[13]- D.M. Leppinen, Trajectory analysis and collision efficiency during Micro bubble flotation, J. of colloid and Interface Science 212, 431-442 (1999)

[14]- Nguyen, A.V., et al , Axisymmetric approach of a solid sphere toward a non-deformable planar interface in the normal stagnation flow- development of global rational approximation for resistance coefficients, Int. J. of Multiphase Flow , 28, 1369-1380 (2002)

[15]- Nguyen, A.V., et al, Sliding of fine particles on the slip surface of rising gas bubbles: Resistance of liquid shear flows, Int. J. of Multiphase Flow, 31, 492-513 (2005)

[16]- Nguyen, A.V. (2007) 'one-step analysis of bubble-particle capture interaction in dissolved-air floatation', In. J. Environment and pollution, Vol. 30, No. 2, 2007

[17]- Nguyen. A.V., Collision Efficiency for fine mineral particles with single bubble in a countercurrent flow regime, Int. J. of Mineral Processing, 35 (1992) 205-223

[18]-M.E Weber and D. Paddock, Interceptional and gravitational collision efficiencies for single collectors at intermediate at intermediate Reynolds numbers, J. of Colloid and Interface Science, 94 (2) (1983) 328-335

[19]-Chi M. Phan et al., Investigation of bubble- particle interactions, Int. J. Miner. Process. 72 (2003) 239-254

[20]-Zongfu Dai. Et al., Particle-bubble collision models-a review, Advances in colloid and interface Science 85 (2000) 231-256

[21]-K.L Sutherland, Physical chemistry factors flotation XI. Kinetics of the flotation process, J. phys. Chem. 52 (1948) 394-425

[22]- Gaudin, A.M., Flotation, 2nd edition. McGraw-Hill, New York, 1957

[23]-Dukhin S.S, Critical value of the Stokes number and the Sutherland formula, Kolloiden. Zh. 45 (2), 207-218

[24]- Zongfu Dai et al., The inertial hydrodynamic interaction of particles and rising bubbles with mobile surfaces, J. of Colloid and Interface Science 197 (1998) 275-292

[25]-Nguyen P et al., Validation of the generalized Sutherland equation for bubble-particle encounter efficiency in flotation: effect of particle density, Minerals Engineering 22 (2009) 176-181

[26]-Nguyen C.M et al., Computational validation of the generalized Sutherland equation for bubble-particle encounter efficiency in flotation, Int. J Miner. Process 81 (2006) 141-148

[27]-C.W. Hirt, B.D. Nichols, Volume of fluid (VOF) method for the dynamics of free boundaries, Journals of Computational physics.39 (1981). Page 201-225

[28]-Brackbill, J.U Kothe, D.B.Zemach, A continuum method for modeling surface tension. Journals of Computational physics 100, 1992, page 335-354

[29]-Stokes, G. C. (1850) Mathematical and Physical papers, volume III, no. 33. Johnson Reprint Corp. (1966)

[30]- Hadamard, J.S. 1911 Mouvement permanent lent d'une sphere liquid et visqueuse dans un liquid visqueux,comptes Rendus Hebdomadaires des séances de V acad des Sci(PARIS), 152, 1735-1738

 [31]- Rybczynski, W. 1911, Uber die fortschreitende bewwegung einer flussigen kugel in einem zahen medium. Bull. Acad. Sci. Cracovie Ser. A1, 40-46

[32]- H. Ström et al., Numerical simulations of solid particle motion in rarefied flow using VOF, Proceeding of the international conference on multiphase flow 2010 (ICMF-2010)

[33]-O. Ubbink, Numerical prediction of two fluid systems with sharp interfaces, Ph.D. Thesis, Imperial College of science, Technology and Medicine, 1997

[34]- T.J. Chung, Computational fluid Dynamics, Cambridge university press, 2002

[35]- D. Rodrigue, Generalized correlation for bubble motion, AIChE Journal, Vol47, No.1, (2001)

[36]- N.M Aybers, A. Tapucu, Studies on the drag and shape of the gas bubble rising through a stagnant liquid, Wärme-und Stoffubertragung 2, 171-177, (1969)

[37]-Leifer et al., A study on the temperature variation of rise velocity for large clean bubbles, Journal of Atmospheric and Oceanic technology, volume 17,1392-1404, (1999)

[38]- N.M Aybers, A. Tapucu, The motion of gas bubble rising through stagnant liquid, Wärme-und Stoffubertragung 2, 118-128, (1969)

 [39]- Schulze.H.J et al. , Investigation of the collision process between particles and gas bubbles in flotation- A Theoretical Analysis, Int. J. of Mineral Processing, 27 (1989) 263-278

[40]-Ralston et al., Inertial hydrodynamic particle-bubble interaction in flotation. Int. J. Miner Process 56, 207-256, 1999

[41]-Levin, L. I., in, Research into the physics of coarsely dispersed aerosols, p.267Isd. Akad, Nauk SSR, Moscow, 1961 [in Russian]

[42]- Yoon R.H, The role of hydrodynamic and surface forces in bubble-particle interaction, Int. J. Miner. Process 58 (2000) 129-143